Food and Chemical Toxicology 135 (2020) 110958

Contents lists available at ScienceDirect

Food and Chemical Toxicology

journal homepage: www.elsevier.com/locate/foodchemtox

Anti-inflammatory effect of nano-encapsulated nerolidol on zymosan-induced arthritis in mice

Eloísa Portugal Barros Silva Soares de Souza[a], Gabriela das Graças Gomes Trindade[a], Marcelo Vinicius Lins Dantas Gomes[a], Luiz André Santos Silva[b], Renata Grespan[b], Lucindo José Quintans Junior[b], Ricardo Luiz Cavalcanti de Albuquerque Júnior[c], Saravanan Shanmugan[a,*], Adriano Antunes de Souza Araújo[a,**]

[a] Department of Pharmacy, Federal University of Sergipe, São Cristóvão, Sergipe, Brazil
[b] Department of Physiology, Federal University of Sergipe, São Cristóvão, Sergipe, Brazil
[c] Institute of Technology and Research, University Tiradentes, Aracaju, Sergipe, Brazil

ARTICLE INFO

Keywords:
Nerolidol
Polymeric nano-capsules
Arthritis
IL-10
IL-1β
TNF-α

ABSTRACT

Nerolidol is naturally occurring sesquiterpene has wide range of biological properties including anti-inflammatory activity. However, it has high volatility with low solubility in nature. The present study aimed to develop and characterized nano-encapsulated nerolidol and evaluated its activity on zymosan-induced arthritis model. Nano-capsules were produced by interfacial deposition of preformed polymer method and characterized by particle size, pH, polydispersity index (PDI), zeta potential, drug content and transmission electron microscopy (TEM). *In vitro* cytotoxicity of formulations was evaluated by alamar blue and MTT assays. *In vivo* neutrophils migration assay was performed on intra-articular zymosan-induced arthritis model in mice. Nano-encapsulated nerolidol suspensions presented adequate properties: mean diameter of particles 219.5 ± 8.4 nm, pH: 6.84 ± 0.5, PDI ≤ 0.2, the zeta potential was −20.3 ± 3.6 mV and drug content 71,2 ± 1.3%. The formulations did not demonstrated cytotoxicity under the conditions assessed. Nerolidol 300 mg/kg inhibited neutrophils migration into joint cavity by 18.8% remains compared with control group, and nano-encapsulated nerolidol 3 mg/kg inhibited (26.7% remains) similar to free nerolidol 10 mg/kg (27.4% remains). Histological, quantification of pro-inflammatory and anti-inflammatory cytokines proves the same results. In conclusion the data suggests that nanoencapsulation of nerolidol improved its anti-inflammatory effect on arthritis in mice.

1. Introduction

Essential oils are well known for their aromatic and biological activities (Sharma et al., 2018). Its chemical compositions are contrast depending on climatic, geographic and distillation techniques. Essential oils are grouped into two main series: the aromatic series are the derivatives of phenylpropane which derived from the metabolism of shikimic acid. Another terpene series originating from mevalonic acid, in which sesquiterpenes (15 carbon atoms) are included (Blowman et al., 2018).

The nerolidol (3,7,11-trimethyl-1,6,10-dodecatrien-3-ol) is a sesquiterpene naturally found in essential oils of various plants, such as: *Ginkgo biloba* L., *Momordica charantia* L., *Baccharis dracunculifolia* DC., *Piper claussenianum* (Miq.) C. DC, *Zanthoxylum hyemale* A.St.-Hil., *Zornia brasiliensis* Vogel, *Swinglea glutinosa* (Blanco) Merr., and others approximately thirty species have content of this essential oil. This unsaturated acyclic alcohol with branched chain has two isomers (cis and trans) and contains a chiral carbon having R and S enantiomers (Chan et al., 2016). This terpene has several biological activities including antiulcerogenic, antitumor, repellent, antioxidant, antinociceptive, anxiolytic, antiparasitic, anti-trypanosomes, anti-leishmania, anti-schistosomal, antimalarial, anti-nematicide, antifungal, permeation

* Corresponding author.Laboratory of Pharmaceutical Assays and Toxicity (LeFT), Department of Pharmacy, Federal University of Sergipe, Av. Marechal Rondon, Jardim Rosa Elze, 49100-000, São Cristóvão, Sergipe, Brazil.
** Corresponding author.
E-mail addresses: eloisaportugal@gmail.com (E.P. Barros Silva Soares de Souza), gabyggt@gmail.com (G.d.G.G. Trindade), luizandressilva@yahoo.com.br (L.A. Santos Silva), grespanrenata@gmail.com (R. Grespan), lucindojr@gmail.com (L.J. Quintans Junior), ricardo.patologia@uol.com.br (R.L. Cavalcanti de Albuquerque Júnior), saranflora04@gmail.com (S. Shanmugan), adriasa2001@yahoo.com.br (A. Antunes de Souza Araújo).

https://doi.org/10.1016/j.fct.2019.110958
Received 5 October 2019; Received in revised form 4 November 2019; Accepted 7 November 2019
Available online 09 November 2019
0278-6915/

promoter, antimicrobial and anti-inflammatory (Chan et al., 2016; De Carvalho et al., 2018) properties.

The anti-inflammatory action deserves to be emphasized its importance, considering the number of diseases triggered and aggravated by the inflammatory processes, as well as the high adverse effects were developed to the patients (Wang et al., 2016). Rheumatoid arthritis is an autoimmune disease characterized by inflammation in the synovial membrane and consequent progressive degradation of the cartilage lining the bones and joints. This disease affects mainly menopausal women and the prevalence in the population is approximately 1%. The estimated drug cost in the world is 20 billion US$ (Oliveira and Fierro, 2018). It is estimated that by 2023 the world market for rheumatoid arthritis drugs is expected to reach 42.8 billion US$ (https://www.ihealthcareanalyst.com/global-rheumatoid-arthritis-drugs-market/). In addition to the high economic costs, pain and loss in the quality of life of the patients, as well as the increased mortality which demonstrate the severity of the disease and constituting a public health problem with socioeconomic consequences (Hayes et al., 2018). The current drug treatment consists of aggressive therapies for the patients. Depending on the stage and severity of the disease NSAIDs, biological agents, antimalarial or disease modifying drugs are used now a days. Small doses of glucocorticosteroids can be used in conjunction with some of these therapies (Ruiz-Miyazawa et al., 2018). Terpenes are representing a class of organic substances that have high anti-inflammatory potential in arthritis. Particularly, modulation of pro-inflammatory cytokines (TNF-α and β, IL-1, IL-1β, IL-6, IL-17, IL-4, IL-10, TGF-β1, and IFN-γ), disease signaling pathways (RANKL, NFKB, MAPK family, COX-2, iNOS, PGE-2, MPP, MPO, c-FOS, Foxp3 and RORγ) and attenuation of arthritis symptoms with a possible inhibition of disease (Carvalho et al., 2019).

Experimental models of rodent arthritis are widely used because they have similarities with the disease in humans, such as inflammatory cell infiltration, joint edema and histopathological changes. The most commonly used arthritogenic agents are Freund's complete adjuvant, bovine type II collagen, antigens, immunocomplexes, and zymosan (Dolati et al., 2016; Mahdi et al., 2017). Zymosan-induced arthritis model is characterized by the release of pro-inflammatory cytokines such as TNF-α, IL-18, IL-1β, and IL-6, hypertrophy of synovial joint and neutrophil recruitment. Those inflammatory conditions are observed similar in the acute phase of rheumatoid arthritis and osteoarthritis (Guazelli et al., 2018).

However, the high hydrophobicity and volatility of the nerolidol may form an obstacle in the constitution of an effective pharmaceutical form for the treatment of rheumatoid arthritis. This issue can be circumvented by the use of nanotechnology, which helps addition to protecting the active principle, can promote its controlled release of drug in the body system, increase the contact surface, and reduce the adverse effects and irritability (Zhang et al., 2013). Polymeric nanospheres containing nerolidol were prepared for the evaluation of the activity against *Trypanosoma evansi* in *in vitro* and *in vivo* oral trials in mice. It was observed that nanoencapsulation increased the therapeutic efficacy of nerolidol (Baldissera et al., 2016) and this is the only study using nanotechnology for the nerolidol compound. Based on the literature, it is necessary to considering the anti-inflammatory action of this terpene as well as need for effective therapies for the treatment of rheumatoid arthritis hence, this present study aimed to develop polymer nanoparticles containing nerolidol and to evaluate its action in arthritis model.

2. Materials and methods

2.1. Chemicals

Nerolidol (molecular weight: 222.37 g/mol) from Sigma-Aldrich® (98% of purity). Poly ε-caprolactone (molecular weight: 80,000 g/mol) and sorbitan monostearate from Sigma-Aldrich® and polysorbate 80 from Henrifarma (SP). Thiazoly Blue Tetrazolium Bromide, Resazurin sodium salt and Triton X-100 from Sigma-Aldrich, Dulbecco Modified Eagle Medium (DMEM) and Fetal bovine serum (FBS) was obtained from Gibco BRL. Zymosan A from Saccharomyces cerevisiae (Sigma-Aldrich®). Phorbol 12-myristate 13-acetate (PMA, Sigma), Quant-iT ™ PicoGreen® DNA Kit (Invitrogen), histopaque 1119 and 1077 from Sigma-Aldrich®. ABTS ELISA Buffer Kit Peprotech®. Ethanol 99.8% P.A. Neon.

2.2. Nanoparticles synthesis and characterization

Polymeric nanocapsules were prepared by the preformed polymer interfacial deposition method, in which the organic and aqueous phases are heated separately, with stirring and after complete solubilization of the components. The organic phase was poured onto the aqueous phase, and the mixture kept under stirring for 10 min at 40 °C as described by Menezes et al. (2017). Subsequently the mixture was concentrated to a final volume of 10 mL in a rotary evaporator. The composition of the organic phase consisted of: poly (ε-caprolactone) (100 mg), sorbitan monostearate (400 mg), acetone (27 ml) and nerolidol (150 mg); and the aqueous phase, for polysorbate 80 (76.8 mg) and distilled water (53 mL). The nerolidol was added after the total solubilization of the organic phase components. It is a racemic mixture of cis and trans, 98% purity, obtained commercially from Sigma-Aldrich®.

2.3. Particle size and zeta potential

Particle diameter determination and polydispersity index (PDI) analysis was performed using the dynamic light scattering technique using a Zennes 3600 model Zenneser ZEN 3600, Malvern, after dilution of the dispersions (500 times, v/v) in filtered water at 0.45 μm Millipore filter. The zeta potential of the nanocapsules containing nerolidol was determined by the measurement of the electrophoretic mobility (Zetas 3600 nano-ZS model, Malvern) after dilution of the dispersions (500 times, v/v) in 10 mM NaCl solution previously filtered through of 0.45 μm millipore membrane.

2.4. Transmission electron microscopy

The morphology of the nanoparticles was evaluated by transmission electron microscopy (TEM; JEM 1200 Exll, operating at 80 K). The nanoparticle suspension was transferred to carbon/Formvar coated grids and stained negatively with uranyl acetate solution (2% w/v). These analyzes were carried out at the Electronic Microscopy Center of the Federal University of Rio Grande do Sul.

2.5. Nerolidol content in nanoparticles

The content of nerolidol in polymer nano-capsule formulations was determined by high performance liquid chromatography (HPLC) and the analytical method validated according to ANVISA RDC No. 899 and subsequently used to quantify the drug. The identification of nerolidol by HPLC was done following the adapted methodology of He and collaborators (He et al., 2016). HPLC analyzes were performed on a Shimadzu® liquid chromatograph equipped with a DGU-20A3 degasser, two LC-20AD pumps, a SIL-20A HT automatic injector, a CTO-20A furnace, a coupled SPDM20Avp diode array detector to a CBM-20A controller system.

The nanoparticle extraction procedure for quantification was as follows: 100 μL of the nanoparticle suspension was added to a 10 mL volumetric flask containing methanol. After 3 h ultrasonic bath, the solution was transferred to a tube and centrifuged at 10,000 RPM for 10 min (20 °C), and an aliquot of the supernatant was filtered through a 0.2 μm membrane filter and injected into the HPLC for the quantification by assess the areas of peaks referring to two isomers and insertion of value into the equation of straight line of the calibration curve of nerolidol at 20 °C.

2.6. Biological assays

2.6.1. Resazurin reduction cell viability assay

To evaluate cell viability by adding the formulations, the resazurin reduction technique was used. Also, known as alamar blue method, is a colorimetric indicator with oxidation properties. It has blue staining and a small intrinsic fluorescence, and when contacted with viable cells, cellular reductases, such as NADH dehydrogenase, reduce resazurin to resorufin, obtaining pink staining and fluorescence. In this way, it is possible to measure whether the substances used interfere in some way with the cellular viability or not.

J774 line cells were cultured in an oven at 37 °C with 5% CO2 in bottles containing (Dulbecco's Modified Eagle's Medium) DMEM medium supplemented with 10% fetal bovine serum (FBS). Cells were trypsinized after washing with Phosphate buffered saline (PBS) and centrifuged. The pellet was resuspended with 1 ml of medium, and, after counting in Neubauer's chamber by tripan blue staining, were plated in transparent 96-well plates.

After adhesion period (24 h), the cells were incubated with the following treatments: polymer-free nano-capsules, polymer nano-capsules containing nerolidol and unencapsulated nerolidol at concentrations 10, 50, 100 μg/mL for 72 h. Two hours before the end of the incubation period, resazurin diluted in PBS at the concentration 0.15 mg/mL was added. As a toxicity control, 0.5% Triton-X 100 was used, and, as viability control, cells were used only with DMEM medium 10% FBS. The resazurin reaction time was 2 h, and the estimated number of cells in each well on the day of reading was 2 x 105 cells.

The readings were performed by absorbance in the SpectraMax® M5 endpoint reader at wavelengths λ = 570 nm and 595 nm, and the quantification method was employed according to the methodology described by Al Nasiry et al. (Al-Nasiry et al., 2007) using the equation:

$$reduction = \frac{(\varepsilon ox\lambda 595 \times A\lambda 570) - (\varepsilon ox\lambda 570 \times A\lambda 595)}{(\varepsilon ox\lambda 570 \times A'\lambda 595) - (\varepsilon red\lambda 595 \times A'\lambda 570)}$$

In the above equation, εoxλ and εredλ are constants given by the molar extinction coefficient at wavelengths of 595 nm and 570 nm, in the oxidized and reduced forms. Aλ represents the absorbance values generated on the plate reading, and Aλ ′, the absorbance in the wells without cells.

2.6.2. MTT reduction cell viability assay

MTT [3-(4,5-dimethylthiazol-2-yl)-2,5-diphenyltetrazolium bromide] reduction assay also used to evaluate cell viability. This compound measures cell viability by the ability of cells to reduce MTT to formazan, making the staining of the wells from yellow to violet. Mitochondrial dehydrogenases of viable cells act by cleaving the triazolium ring of MTT. This reaction generates crystals of formazan, an insoluble compound of violet coloration. In this way, it is possible to measure the toxicity of a substance through its action on cellular viability.

The same way and conditions in alamar blue assay were used in MTT assay to confirm the test in J774 cell line. Four hours before the end of the incubation time (72 h) MTT solution in PBS at the final concentration in the 0.5 mg/mL was added in each well. After the end of the incubation period, formation of formazan crystals was observed at the bottom of the wells and, when diluted with DMSO, showed purple staining, unlike the wells with triton-x 100, whose dead cells were unable to reduce MTT (Grela et al., 2015). The reading was taken at wavelength λ = 570 nm on a SpectraMax® M5 plate reader. The values were normalized as a function of the control for purposes of quantification as a percentage in the graph.

2.6.3. Ethical aspects

All proposed experimental protocols comply with the ethical criteria of animal experimentation recommended by the Brazilian Society of Laboratory Animal Science (SBCAL) and procedures and care for the handling of animals will be carried out according to the International Association for the Study of Pain. This project was approved by the Animal Research Ethics Committee (CEPA) of the Federal University of Sergipe (22/2018).

2.6.4. Neutrophil migration assay

The *in vivo* assay was performed using 27–30g and 8-weeks-old female Swiss mice. All the experimental animals obtained from the Department of Physiology of the Federal University of Sergipe (São Cristóvão, Brazil) and transferred to the animal house of the Pharmacology Laboratory of the Inflammatory Process. The animals were randomly divided into eight groups, in polypropylene box with 33 cm wide by 40 cm long and 15 cm deep. The packaging was made in a temperature-controlled rack (21 °C), air exhaust system and light/dark cycle of 12/12 h.

The mice were submitted to intra-articular injection of Zymosan (100μg/10 μL) in the femorotibial joint for the induction of arthritis under inhalation anesthesia with halothane (0.01%) (Silva et al., 2018). Thirty minutes previously, treatments with nerolidol had been administered intraperitoneally at doses ranging from 3 mg/kg to 300 mg/kg, controls with saline and the reference drug, indomethacin, at a dose of 5 mg/kg.

Four hours after administration of zymosan, the animals were euthanized, and synovial fluid was withdrawn from the intra-articular joint, further diluted with PBS and stained with the Turk dye. Neutrophils were counted in Neubauer's chamber, and the results expressed as percentage of neutrophil migration to the intra-articular cavity after the inflammatory stimulus, indicating a reduction or not of the compound tested in relation to the zymosan and intraperitoneal saline control.

2.6.5. NET formation assay

To evaluate and quantify the formation of NETs (neutrophil extracellular traps), female neutrophils were used in the marrow neutrophils and the Quant-iT ™ PicoGreen® DNA Kit (Invitrogen) was used. Eight-week-old female Swiss mice were euthanized and the bone marrow from the femur and tibia were extracted using syringes and RPMI medium. The cells were centrifuged and resuspended in RPMI (1640) (Roswell Park Memorial Institute) medium supplemented with 10% or FBS and the neutrophils were separated by the addition of histopaque® (1119 and 1077) which separated the cell types according to the gradient. After the total and differential count, which showed a majority of neutrophils, these were plated in 96-well plates. Different concentrations of Nerolidol were added (1 μM, 10 μM, 50 μM and 100 μM) and incubated for 6 h at 37 °C, 5% CO2.

One hour before the end of the incubation period, 10 nM Phorbol 12-myristate 13-acetate (PMA, Sigma®) was added to induce the formation of NETs. After completion of the 6-h incubation, the cells were centrifuged at 300 rpm for 5 min and 4 °C, and the supernatant was removed and transferred to another 96 well plate where the 10 μM PicoGreen DNA dye was added. After 5 min, reading was done by fluorescence in plate reader (Synergy HT®, Biotek) at 484 nm and 520 nm wavelengths of excitation and emission respectively.

2.6.6. Histological analysis

For histological analysis of the tissues, the animals treated with nerolidol and nanoparticles before 30 min of zymosan induction and every 4 h intervals up to 24 h were euthanized and the intra-articular cavity was removed and transferred to a 0.8% nitric acid solution for 48 h for descaling. The tissues were then dehydrated in increasing concentrations of ethanol 70%, 80%, 90% and absolute ethanol respectively. Continuously, the tissues were treated with xylol for paraffin embedding. The blocks were cut into a microtome and the sections were stained with hematoxylin/eosin (HE) and analyzed under a Euromex optical microscope at increases of 40x to 800x.

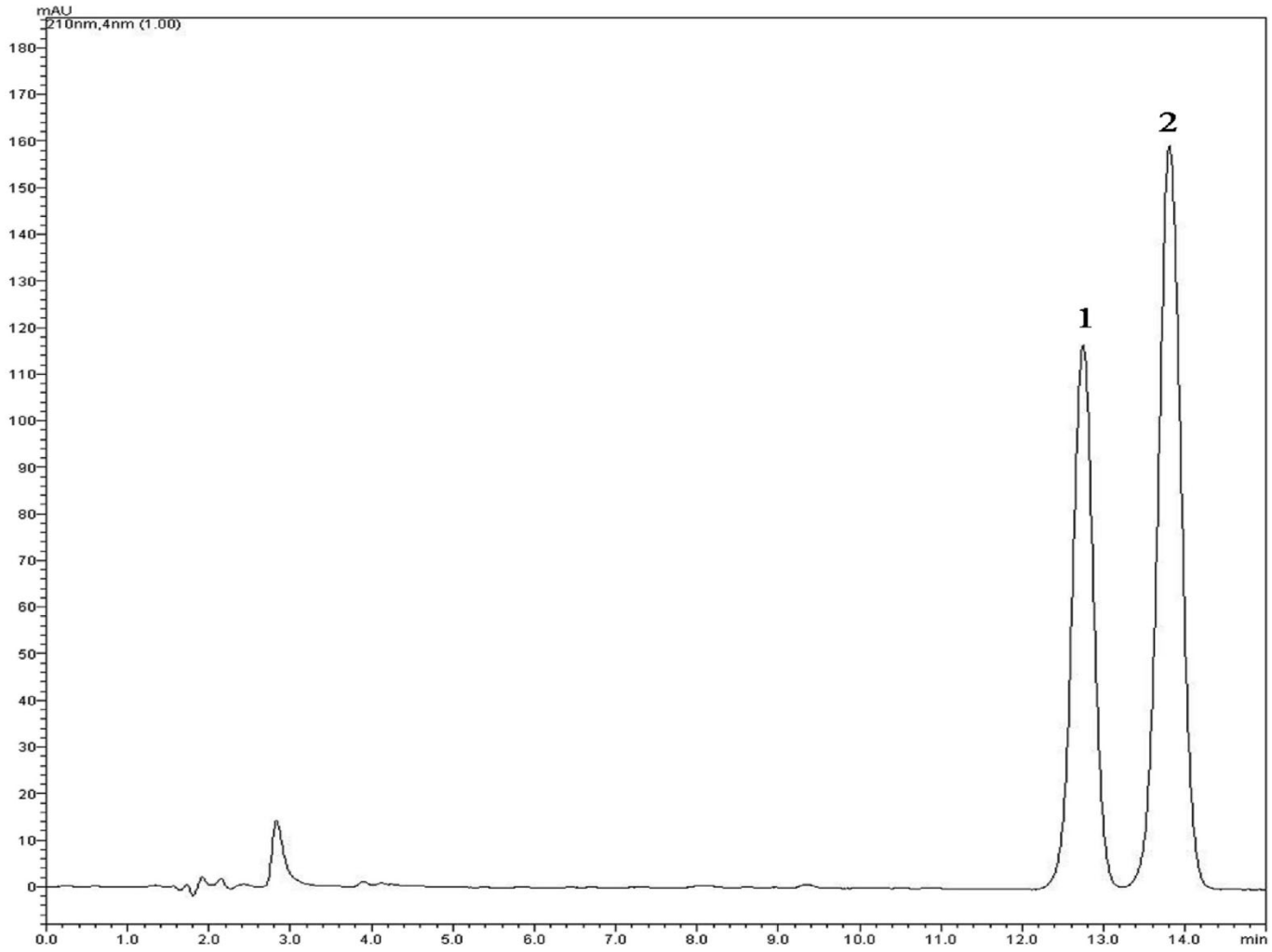

Fig. 1. Representative chromatogram of cis (1) and trans (2) nerolidol. Column C18 (150 × 4.6 mm) and mobile phase methanol/water (80:20) in isocratic elution.

2.6.7. Quantification of inflammatory cytokines by ELISA assay

In order to evaluate the pro-inflammatory and anti-inflammatory cytokines involved in the mechanism of action of nerolidol on synovial inflammation, after the procedure described in neutrophil migration assay, the joint tissue of the mice was removed, crushed and centrifuged, and the supernatant were collected in order to quantifying the ani-inflammatory cytokines IL-10 and pro inflammatory cytokines IL-1β and TNF-α by ELISA assay (Enzyme-Linked Immunosorbent Assay) according to the manufacturer's specifications of the detection Peprotech kit following the methodology of Yamada et al. (2013).

2.7. Statistical analysis

Statistical analyzes were performed using the GraphPad Prism program (version 5). Data graphics were analyzed using the ANOVA variance analysis, followed by the Tukey post-test. The results are expressed as mean ± SD, with a significance level of $p < 0.05$.

3. Results and discussion

Initially, to evaluate the anti-inflammatory activity of nerolidol as well as its nanoencapsulation was complete, followed by nerolidol identification and its encapsulated nanoparticles characterization was done further. The formulations were then tested for potential toxicity in lineage cells in two cell viability assays and further, *in vivo* assays also were carried out: neutrophil migration, histopathological analysis, and evaluation of possible mechanisms involved in NETs formation and action on the main inflammatory mediators.

Nerolidol identification was done by HPLC with approximate retention times of 13 and 14 min for cis and trans isomers respectively (Fig. 1). The linear equation of the compound was $y = 32559x + 34136$, and $R^2 = 0.9995$. These data are consistent with that previous observed study by He and collaborators, which confirming the viability of the method (He et al., 2016). The obtained results prove that purity of the nano encapsulated nerolidol compound, the linear equation also suggest that the nerolidol compound soluble with in the nano encapsulation and the obtained peaks in two retention times confirms it's cis and trans isomers of the nerolidol compound.

The particle size results of nanoparticles containing nerolidol shows particle diameter of 219 ± 8.4 nm. Further, the zeta potential (−20.3 ± 3.6 mV), PDI (0.11 ± 0.02), pH (6.84 ± 0.5) and drug solubility (71.3 ± 1,2%) was observed in the nerolidol encapsulated nanoparticle. These data correspond to the means of analysis of three determinations on three different days. Such analyzes indicate the nanometric size of the particles and their stability in suspension. Further, transmission electron microscopy demonstrated the spherical shape of the nanoparticles and confirmed their nanometric size, as shown in Fig. 2. All these results reveal that the nerolidol compound well encapsulated with the nanoparticles.

The cell viability assay by reducing resazurin showed that the cells remained viable, with resazurin reduction percentage comparable to the control, when treated with the following doses of 10, 50 and

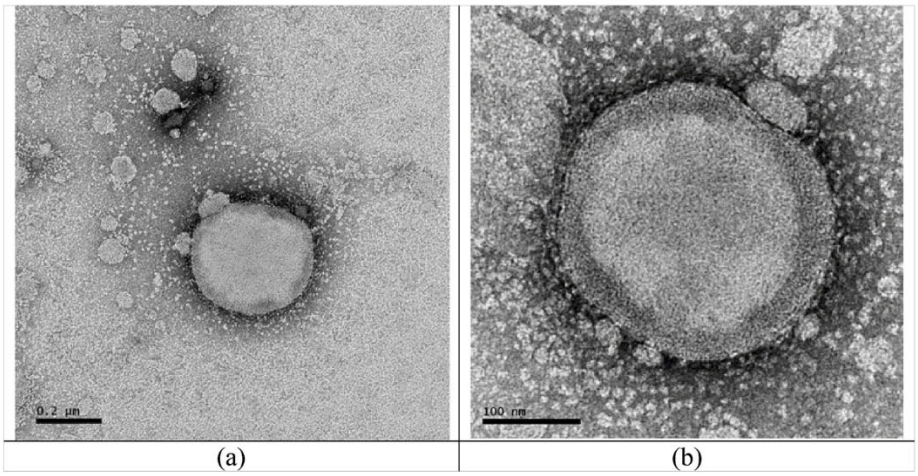

Fig. 2. Transmission electron microscopy of polymeric nanoparticles containing nerolidol, in the increment of 100k (a) and 300k (b).

100 µg/mL the compound: non-drug polymeric nanoparticles (NA), unencapsulated nerolidol (NE) and nerolidol polymer nanoparticles (NN). The results of the experiments in cell J774 is shown in Fig. 3A. This is an indication that the formulations may not present toxicity to the cells as they do not interfere with their viability. This result was confirmed by MTT assay (Fig. 3B). As observed in the results, the MTT reduction percentage calculated from the absorbance values in the control wells was approximately 94% and the treatments varied between 90% and 95%, thus not demonstrating a significant difference between wells treated with nerolidol and nanoparticles, and untreated wells, while the Triton-X 100 control presented a viability percentage of 6%.

The J774 cell line is derived from rat macrophages and is widely used in biological assays. The use of this lineage is justified because the

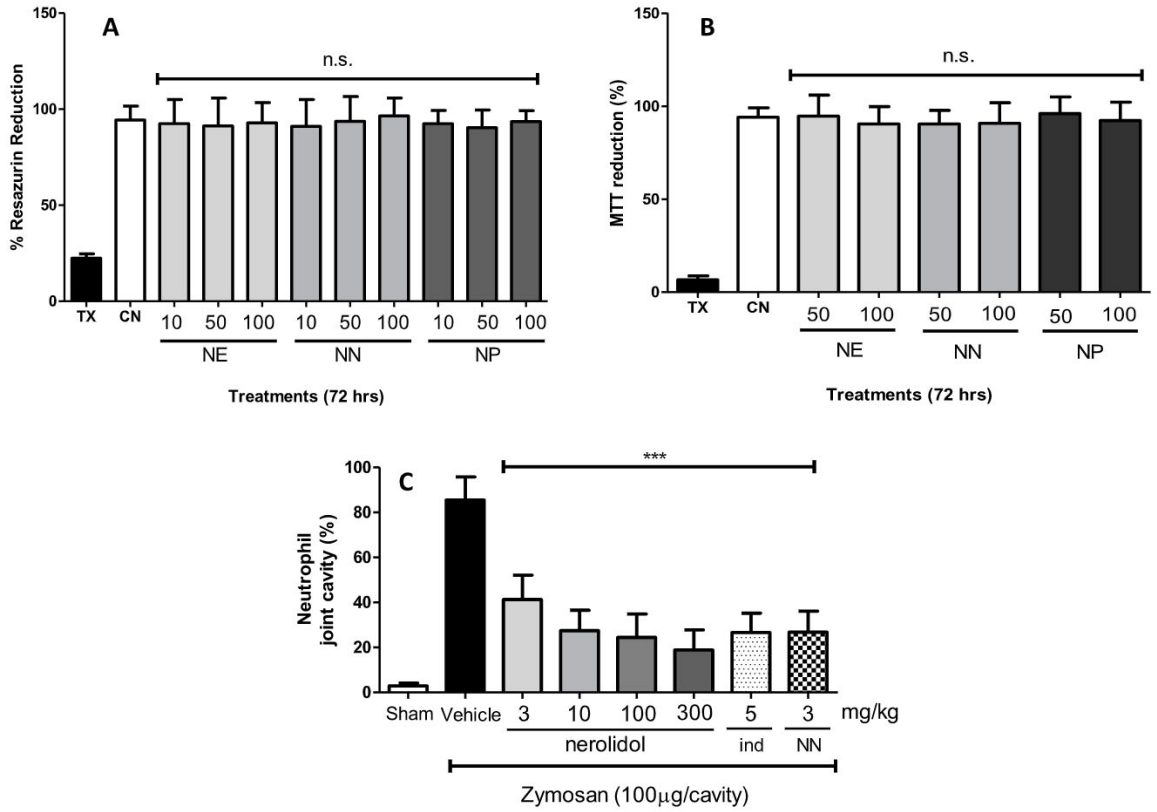

Fig. 3. a) Cell viability assay by reduction of resazurin. Cell linage: J774, incubation time: 72 h, NE: nerolidol free, NN: nerolidol nanoparticles, NP: nanoparticles without nerolidol, TX: triton-X 100 0,5%, 5 min, CN: control DMEM 10% FBS without treatment. n = 5, triplicate. ANOVA $p < 0.05$, Tukey post-test *** IC: 95%. **b)**Cell viability assay by reduction of MTT. Cell linage: J774, incubation time: 72 h, NE: nerolidol free, NN: nerolidol nanoparticles, NP: nanoparticles without nerolidol, TX: triton-X 100 0,5%, 5 min, CN: control DMEM 10% FBS without treatment. n = 5, triplicate. ANOVA $p < 0.05$, Tukey post-test *** IC: 95%. **c)**In vivo assay of neutrophil migration into the joint cavity. Female Swiss mice were treated with nerolidol and nanoparticles intraperitoneally 30 min prior to intra-articular zymosan injection. 4 h later mice were euthanized and the peritoneal lavage was counted in the neubauer chamber. Sham: mice did without zymosan induction, saline intra-articular, Vehicle: animals treated with vehicle: saline, ethanol 0,5%, tween 80 0,5%, Ind: indomethacin, NN: nerolidol loaded nanoparticles. n = 15, five animals per group in three different days. ANOVA $p < 0.05$, Tukey post-test *** IC: 95%.

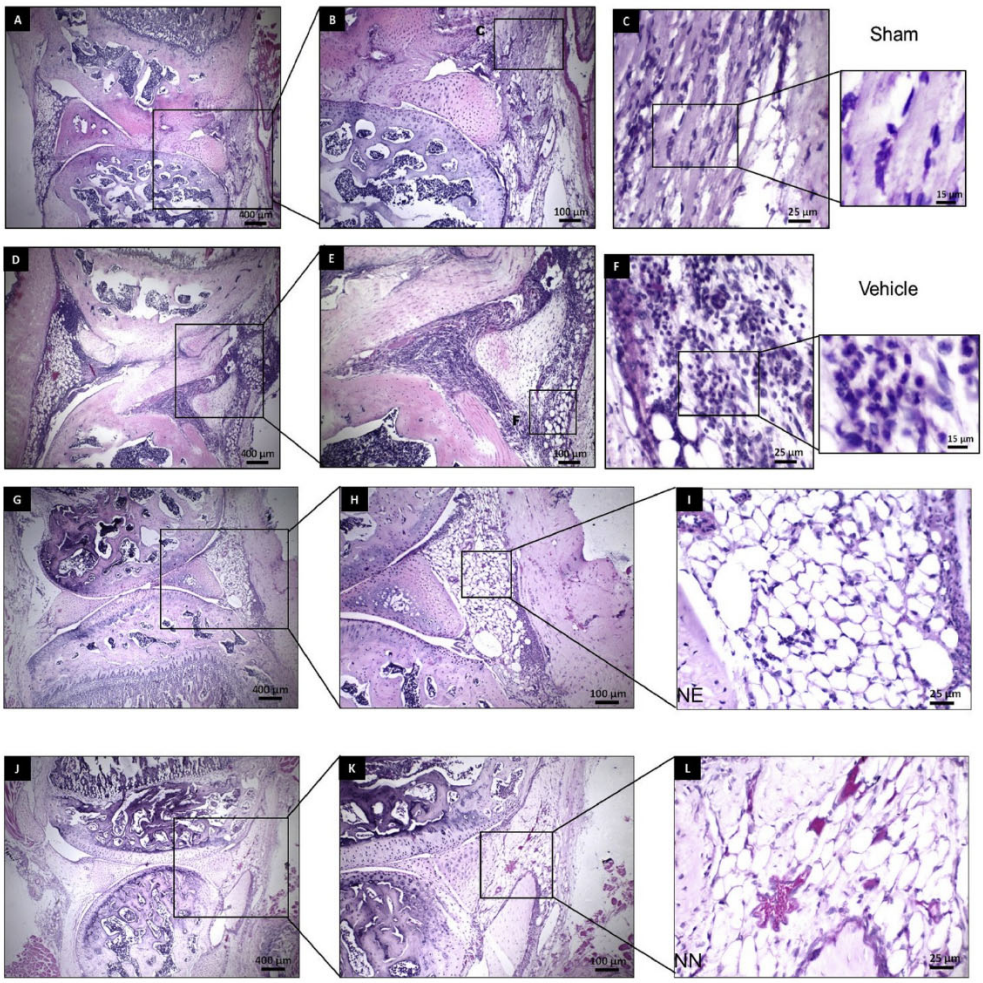

Fig. 4. Photomicrographs of histological sections stained in HE representative of the femoral-tibial joint of Swiss mice. Sham group: animals without induction by zymosan, i. a. saline injection. Panoramic view (A, 40×) discrete inflammatory infiltrate and mild interstitial edema. Anterior region (B, 100x) with discrete lymphocytic infiltrate (C, 400x) and possible neutrophils. Vehicle group: animals with induction of zymosan treated i. p. with vehicle (saline, ethanol 0,5% and tween 80 0,5%). A panoramic view (D, 40×) showing intense inflammatory infiltrate in the anterior and posterior (E, 100×) of the joint, with infiltrate rich in neutrophil polymorphonuclear cells and macrophages (F, 400×). The largest magnifications bring details of the intense neutrophilic inflammatory infiltrate (800×). NE group: induction with zymosan and treatment intraperitoneally with nerolidol 3 mg/kg every 4 h. Panoramic view (G, 40x) showing moderate inflammatory infiltrate, more expressive than the NN group and at lower intensity than in the CP group. Anterior region (H, 100x) with presence of edema and partially controlled neutrophil and lymphocyte infiltrate (I, 400x). NN group: induction with zymosan and treatment i. p. with nerolidol-loaded nanoparticles 3 mg/kg every 4 h. Panoramic view (J, 40×) slightly inflamed synovial membrane, posterior region (K, 100x) with controlled inflammatory foci, (L, 400x) preserved adipose cushion with presence of some neutrophils and lymphocytes.

macrophages are the first line of defense of the organism and a cellular type distributed throughout the tissues (Sharma et al., 2016). Cell viability assays have this dual function according to the purpose of the experiment. Alamar blue and MTT can be used both to demonstrate the safety of a compound or nanoparticle formulation (Huang et al., 2016) for lack of toxicity, and to demonstrate its toxicity to antitumor activity or to some specific pathogen (Ambrož et al., 2015).

Neutrophils are the predominant type of immune cell in the joint cavity and synovial fluid of patients with arthritis. Cartilage degradation, release of reactive oxygen species and inflammatory mediators such as lysosomal enzymes and metalloproteases in rheumatoid arthritis are a consequence of the accumulation of neutrophils in the region (Rosas et al., 2015). In the *in vivo* assay, it was observed that nerolidol alone showed a dose-dependent effect. At the dose of 300 mg/kg reduced the neutrophil migration in to the joint cavity (18.8% remains) compared to control group animals (total 85.5%). Meanwhile, the dose of 3 mg/kg, also inhibit the local inflammation (41.3% remains), which is also a significant result compare to the control (Fig. 3C) group. Meantime, the suspension of nano-encapsulated nerolidol in the same 3 mg/kg dose was tested for comparison purposes. The obtained results revealed nano-encapsulated nerolidol significantly reduced neutrophil migration (26.7% remains) which is equal to the result of standard drug indomethacin (26.6% remains) and free nerolidol 10 mg/kg (27.4% remains). The dose-response curve experiment showed that 2.3 mg/kg of nerolidol is significantly inhibit (ID_{50} Inhibitory dose) the 50% of neutrophils. Analysis of the neutrophil migration graph demonstrates that the zymosan arthritis induction model works in promoting inflammation in the joint cavity. It is also observed that free nerolidol considerably reduced acute inflammation. Fonseca et al. evaluated that orally administrated nerolidol 200, 300 and 400 mg/kg significantly inhibit neutrophil migration at 57% in a higher dose (Fonsêca et al., 2016). Similar studies were performed previously for the neutrophil migration assays, which evaluated the effect of *Schinus terebinthifolius* hydroalcoholic extract and the estrogen *Tamoxifen versus* zymosan induction (Rosas et al., 2015; Silva et al., 2018). Our present results exhibit higher results when compared to these previous reports.

The low solubility of terpenes due to their chemical structure limits its use in the biological activities. Focused on this fact, the use of nanotechnology tends to overcome this problem in addition to reducing the amount of drug administration (Dolati et al., 2016). This property was observed earlier by Nagai et al. (Nagai and Ito, 2014) in preparation of indomethacin solid nanoparticles allowed a considerable reduction in the administration of the dose. Also, in our present study, the improvement of drug potency was observed, in which encapsulated nerolidol at the dose of 3 mg/kg have effective activity when compared to 10 mg/kg of free nerolidol. The histological changes of the sham group showed mild lymphocytic inflammatory infiltration, with some few macrophages and polymorphonuclear neutrophil cells, within delicate connective tissue. In the vehicle group, an intense inflammatory infiltration predominantly consists polymorphonuclear neutrophil cells (acute inflammation) and occasional macrophages and lymphocytes. Also, areas of intense interstitial edema and severe serofibrinous exudation were observed (Fig. 4). Meanwhile, the synovial membrane of the animals treated with nerolidol and nanoencapsulated nerolidol (NE and NN groups) revealed reduction of inflammatory infiltration and edema in both groups. These pathological features confirm that anti-inflammatory activity of nerolidol in the *in vivo* neutrophil migration

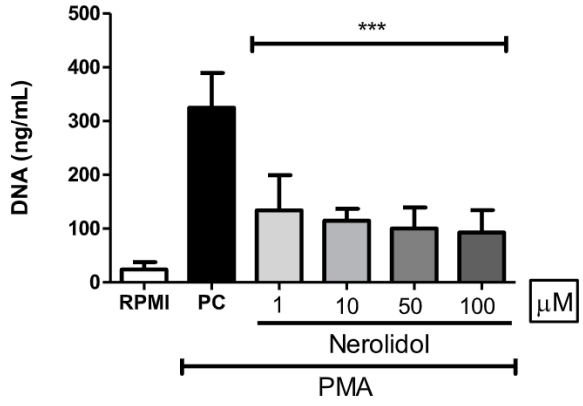

Fig. 5. In vitro NETs formation in medullar neutrophil. Swiss mice were euthanized and bone marrow extracted after neutrophil separation steps were incubated for 6 h with nerolidol. PMA acted for 1 h inducing the formation of NETs, which was quantified by the Picogreen fluorescent dye in the cell culture supernatant. n = 3, triplicate. ANOVA $p < 0.05$, Tukey post-test *** IC: 95%.

assay and points out at a possible improvement of such biological effect provided by the nanoencapsulated nerolidol. Previous studies have demonstrated that infiltration of inflammatory cells as a result of zymosan-induced arthritis is greater in the first 24 h, tends to decrease after 3 and 7 days, and then it is replaced by a synovial hyperplasia (Hashimoto et al., 2018). As intraperitoneal introduction of nerolidol exhibits a peak plasma concentration at after 20th minutes of its administration and it is eliminated from the body within 24 h (He et al., 2016), the development of the current formulation aimed to treat inflammation in an acute model. Pathological analyzes of other works using the knee joint in a model of intra-articular inflammation induced by zymosan confirm the viability of the method. The crude aqueous extract of the plant species *Libidibia ferrea* 200 mg/kg orally administered in animals subjected to intra-articular injection of zymosan promoted reduction of the inflammatory parameters in the synovial membrane when compared to the intense leukocyte infiltrate and fibrosis observed in the control group without treatment (Falcão et al., 2019). In addition, intraperitoneal administration of 30 μg of the *Coccidioides posadasii* extract resulted in decrease in the synovial cell hyperplasia, fibrosis and neovascularization (Pinto et al., 2013). Our results also produced better activity when compared to all these previous reports.

In previous literature, there is no studies were found on the activity of nerolidol in the arthritis model. Therefore, this is the first study besides confirming the anti-inflammatory action of nerolidol in the arthritis model for this terpene compound. Added to the use of nanotechnology for potentialization of the effect, in agreement with the studies of Baldissera et al. (2016) but using another pathway and different biological activity.

With the objective of identify the possible mechanisms involved in reducing the inflammatory response promoted by nerolidol in the arthritis model, *in vivo* and *in vitro* experiments were performed. The NETs assay is based on the quantification of extra cellular DNA by the Picogreen fluorescent dye. The induction of NET formation occurs through the action of PMA, an ester that has specific action on protein kinase C and NF-κB. In neutrophils, exposure to PMA induces the release of chromatin fibers decorated with myeloperoxidase, neutrophil elastase and antimicrobial proteins (Masuda et al., 2017). Thus, it was possible to observe through the fluorescence values a high DNA labeling in the supernatant medium of the cells treated with PMA, and a reduction in the wells treated with nerolidol. These data may indicate one of the possible mechanisms by which nerolidol acts in reducing the inflammatory picture in arthritis models. The reduction in NET formation by nerolidol was significant (Fig. 5) and indicates one of the mechanisms by which this terpene acts at the cellular level. The elucidation of the inflammatory pathways involved in the mechanism of action of the drug is important for the discovery of possible adverse effects and of which other drugs it can be co-administered (Papayannopoulos, 2018). Khandpur et al. observed the NETosis process in circulating neutrophils of synovial fluid induced by inflammatory cytokines IL-17A and TNF-α (Khandpur et al., 2013).

Further, the mechanism of the rheumatoid arthritis inflammation process was confirmed with the analysis of cytokines and interleukins such as TNF-α, IL-1β and IL-10. Fig. 6 demonstrate that the results of the proinflammatory cytokine TNF-α, IL-1β and anti-inflammatory cytokine IL-10, which reveals that animals treated with nerolidol, nano-encapsulated nerolidol and indomethacin drugs enhanced the TNF-α, IL-10 and IL-1β when compared to the vehicle group which induce the arthritis only. Especially, in the anti-inflammatory cytokine IL-10 level of vehicle group reduced by the zymosan-induced arthritis condition but in the nerolidol alone, nano-encapsulated nerolidol and indomethacin drugs improves the IL-10 it reveals increasing anti-inflammatory cytokine in the inflammatory site also controls the pro-inflammatory cytokines and reduces the arthritis condition. Based on results the TNF-α level of the treated animals were similarly same in sham, vehicle and nano-encapsulated nerolidol group but in the indomethacin and only nerolidol increased the TNF-α level. The synovial membrane in patients with RA is characterized by hyperplasia, proliferation, angiogenesis and an infiltrate of predominantly $CD4^+$ T helper (Th) cells. The pro-inflammatory cytokines, especially tumor necrosis factor alpha (TNF-α), and two interleukins are the key cytokines which drive inflammation and the destructive process (Müller et al., 2008; Khandpur et al., 2013). TNF-α play a vital role in the pathogenesis of osteoarthritis (OA) and rheumatoid arthritis. Beside these pro-inflammatory cytokines associated with OA, the immunoregulatory cytokine IL-10 has been shown to be elevated in osteoarthritic cartilage and synovium, IL-10 is a pleiotropic cytokine that has immunoregulatory properties regulating macrophage, T cell, dendritic cell and natural killer cell functions (Feldmann et al., 1996; Isomäki and Punnonen, 1997; Müller et al., 2008). The TNF-α mediated down-regulation of aggrecan expression was significantly antagonized by IL-10 overexpression, which modulates some catabolic features of TNF-α in chondrocytes of the arthritis side (Müller et al., 2008). The reduction of the pro-inflammatory cytokine IL-1β also one of the main reasons for the improvement of the anti-inflammatory cytokine IL-10. In rheumatoid arthritis, IL-1β propagates the synthesis of cyclooxygenase (COX)-2 which triggers the release of prostaglandin E2 (PGE2) (Dinarello, 2002). Therefore, the inhibition of IL-1β level by the nerolidol and nano-encapsulated nerolidol group might be reduce the (COX)-2 enzyme level and also demote the release of PGE2 which control the arthritis also the TNF-α and IL-1β might be the inhibit by the reduction og the $CD4^+$ T helper (Th) cells. In this present study the obtained results by the nerolidol and its nano-encapsulated drug could be functioned on the same above-mentioned all mechanism and reduced the rheumatoid arthritis condition.

4. Conclusion

The results point to a significant inhibition of inflammation in the joint cavity of arthritis was observed by free nerolidol and its polymer nanoparticles. Particularly, both products inhibit the disease condition by improving the anti-inflammatory cytokine level and significantly inhibits the neutrophil migration into the joint cavity. Further, the histological observation also proves that edema, neutrophil and lymphocyte infiltration are clearly controlled by the free nerolidol and its polymer nanoparticles compound. These findings reported here, should help to evaluate further research whether this monoterpene compound has protective therapeutic approach to prevent joint inflammation developed by the arthritis in the clinical aspects.

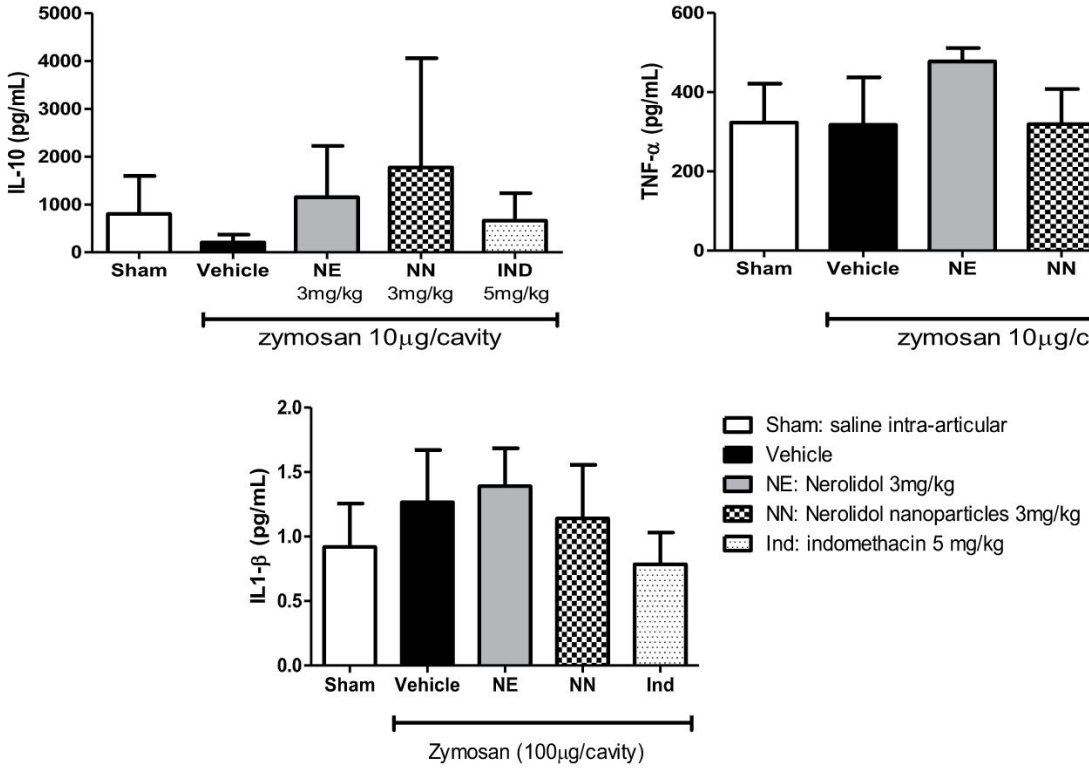

Fig. 6. Effect of nerolidol on inflammatory cytokine release IL-10, TNF-α and IL-1β in ELISA assay. n = 5. ANOVA $p < 0.05$, Tukey post-test, IC: 95%.

Declaration of competing interest

The authors declare that they have no known competing financial interests or personal relationships that could have appeared to influence the work reported in this paper.

Acknowledgments

We are grateful to Luiz Anastácio Alvez and Laboratório de Comunicação Celular from Fundação Oswaldo Cruz of Rio de Janeiro, and Centro de Nanociência e Nanotecnologia from Federal University of Rio Grande do Sul for assit the lab facilities. We are also grateful to the laboratory staff Laboratório de Ensaios Farmacêuticos e Toxidade (Left), Laboratório Integrado de Biologia Experimental (Libex), Laboratório de Morfologia e Patologia Experimental (LMPE) for their support. We thank for the financial support from CAPES, CNPq and FAPITEC-SE.

Appendix A. Supplementary data

Supplementary data to this article can be found online at https://doi.org/10.1016/j.fct.2019.110958.

References

Al-Nasiry, S., Geusens, N., Hanssens, M., Luyten, C., Pijnenborg, R., 2007. The use of Alamar Blue assay for quantitative analysis of viability, migration and invasion of choriocarcinoma cells. Hum. Reprod. 22, 1304–1309. https://doi.org/10.1093/humrep/dem011.

Ambrož, M., Boušová, I., Skarka, A., Hanušová, V., Králová, V., Matoušková, P., Szotáková, B., Skálová, L., 2015. The influence of sesquiterpenes from myrica rubra on the antiproliferative and pro-oxidative effects of doxorubicin and its accumulation in cancer cells. Molecules 20, 15343–15358. https://doi.org/10.3390/molecules200815343.

Baldissera, M.D., Grando, T.H., Souza, C.F., Cossetin, L.F., Sagrillo, M.R., Nascimento, K., da Silva, A.P.T., Dalla Lana, D.F., Da Silva, A.S., Stefani, L.M., Monteiro, S.G., 2016. Nerolidol nanospheres increases its trypanocidal efficacy against Trypanosoma evansi: new approach against diminazene aceturate resistance and toxicity. Exp. Parasitol. 166, 144–149. https://doi.org/10.1016/j.exppara.2016.04.015.

Blowman, K., Magalhães, M., Lemos, M.F.L., Cabral, C., Pires, I.M., 2018. Anticancer properties of essential oils and other natural products. Evidence-based complement. Altern. Med. https://doi.org/10.1155/2018/3149362.

Carvalho, A.M.S., Heimfarth, L., Santos, K.A., Guimarães, A.G., Picot, L., Almeida, J.R.G.S., Quintans, J.S.S., Quintans-Júnior, L.J., 2019. Terpenes as possible drugs for the mitigation of arthritic symptoms - a systematic review. Phytomedicine 57, 137–147. https://doi.org/10.1016/j.phymed.2018.10.028.

Chan, W.-K., Tan, L.T.-H., Chan, K.-G., Lee, L.-H., Goh, B.-H., 2016. Nerolidol: a sesquiterpene alcohol with multi-faceted pharmacological and biological activities. Molecules 21. https://doi.org/10.3390/molecules21050529.

De Carvalho, R.B.F., De Almeida, A.A.C., Campelo, N.B., Lellis, D.R.O.D., Nunes, L.C.C., 2018. Nerolidol and its pharmacological application in treating neurodegenerative diseases: a review. Recent Pat. Biotechnol. 12, 158–168. https://doi.org/10.2174/1872208312666171206123805.

Dinarello, C.A., 2002. The IL-1 family and inflammatory diseases. Clin. Exp. Rheumatol. 20, S1–S13.

Dolati, S., Sadreddini, S., Rostamzadeh, D., Ahmadi, M., Jadidi-Niaragh, F., Yousefi, M., 2016. Utilization of nanoparticle technology in rheumatoid arthritis treatment. Biomed. Pharmacother. 80, 30–41. https://doi.org/10.1016/j.biopha.2016.03.004.

Falcão, T.R., Rodrigues, C.A.O., De Araújo, A.A., De Medeiros, C.A.C.X., Soares, L.A.L., Ferreira, M.R.A., Vasconcelos, R.C., De Araújo Júnior, R.F., De Sousa Lopes, M.L.D., Guerra, G.C.B., 2019. Crude extract from Libidibia ferrea (Mart. ex. Tul.) L.P. Queiroz leaves decreased intra articular inflammation induced by zymosan in rats. BMC Complement Altern. Med. https://doi.org/10.1186/s12906-019-2454-3.

Feldmann, M., Brennan, F.M., Maini, R.N., 1996. Role of cytokines in rheumatoid arthritis. Annu. Rev. Immunol. 14, 397–440. https://doi.org/10.1146/annurev.immunol.14.1.397.

Fonsêca, D.V., Salgado, P.R.R., de Carvalho, F.L., Salvadori, M.G.S.S., Penha, A.R.S., Leite, F.C., Borges, C.J.S., Piuvezam, M.R., Pordeus, L.C. de M., Sousa, D.P., Almeida, R.N., 2016. Nerolidol exhibits antinociceptive and anti-inflammatory activity: involvement of the GABAergic system and proinflammatory cytokines. Fundam. Clin. Pharmacol. 30, 14–22. https://doi.org/10.1111/fcp.12166.

Grela, E., Ząbek, A., Grabowiecka, A., 2015. Interferences in the optimization of the MTT assay for viability estimation of Proteus mirabilis. Avicenna J. Med. Biotechnol. (AJMB) 7, 159–167.

Guazelli, C.F.S., Staurengo-Ferrari, L., Zarpelon, A.C., Pinho-Ribeiro, F.A., Ruiz-Miyazawa, K.W., Vicentini, F.T.M.C., Vignoli, J.A., Camilios-Neto, D., Georgetti, S.R., Baracat, M.M., Casagrande, R., Verri, W.A., 2018. Quercetin attenuates zymosan-induced arthritis in mice. Biomed. Pharmacother. 102, 175–184. https://doi.org/10.1016/j.biopha.2018.03.057.

Hashimoto, K., Oda, Y., Nakagawa, K., Ikeda, T., Ohtani, K., Akagi, M., 2018. LOX-1 deficient mice show resistance to zymosan-induced arthritis. Eur. J. Histochem. 62, 2847. https://doi.org/10.4081/ejh.2018.2847.

Hayes, C.J., Payakachat, N., Li, C., 2018. Evaluation of opioid use among patients with back disorders and arthritis. Qual. Life Res. 27, 3021–3035. https://doi.org/10.1007/s11136-018-1941-1.

He, Y.S., Sun, W., Zhang, B.Y., Xu, L.H., Yang, J., Gao, W., Qi, L.W., Li, P., Wen, X.D., 2016. Application of a sensitive liquid chromatography-mass spectrometry method to a pharmacokinetic study of nerolidol in rat plasma. Anal. Methods. https://doi.org/10.1039/c5ay02575c.

Huang, P.-H., Hu, S.C.-S., Lee, C.-W., Yeh, A.-C., Tseng, C.-H., Yen, F.-L., 2016. Design of acid-responsive polymeric nanoparticles for 7,3',4'-trihydroxyisoflavone topical administration. Int. J. Nanomed. 11, 1615–1627. https://doi.org/10.2147/IJN.S100418.

Isomäki, P., Punnonen, J., 1997. Pro- and anti-inflammatory cytokines in rheumatoid arthritis. Ann. Med. 29, 499–507.

Khandpur, R., Carmona-Rivera, C., Vivekanandan-Giri, A., Gizinski, A., Yalavarthi, S., Knight, J.S., Friday, S., Li, S., Patel, R.M., Subramanian, V., Thompson, P., Chen, P., Fox, D.A., Pennathur, S., Kaplan, M.J., 2013. NETs are a source of citrullinated autoantigens and stimulate inflammatory responses in rheumatoid arthritis. Sci. Transl. Med. 5 (178ra40). https://doi.org/10.1126/scitranslmed.3005580.

Mahdi, H.J., Khan, N.A.K., Asmawi, M.Z. Bin, Mahmud, R., A/L Murugaiyah, V., 2017. In vivo anti-arthritic and anti-nociceptive effects of ethanol extract of Moringa oleifera leaves on complete Freund's adjuvant (CFA)-induced arthritis in rats. Integr. Med. Res. https://doi.org/10.1016/j.imr.2017.11.002.

Masuda, S., Shimizu, S., Matsuo, J., Nishibata, Y., Kusunoki, Y., Hattanda, F., Shida, H., Nakazawa, D., Tomaru, U., Atsumi, T., Ishizu, A., 2017. Measurement of NET formation in vitro and in vivo by flow cytometry. Cytometry 91, 822–829. https://doi.org/10.1002/cyto.a.23169.

Menezes, P.D.P., Frank, L.A., Lima, B.D.S., de Carvalho, Y.M.B.G., Serafini, M.R., Quintans-Júnior, L.J., Pohlmann, A.R., Guterres, S.S., Araújo, A.A. de S., 2017. Hesperetin-loaded lipid-core nanocapsules in polyamide: a new textile formulation for topical drug delivery. Int. J. Nanomed. 12, 2069–2079. https://doi.org/10.2147/IJN.S124564.

Müller, R.D., John, T., Kohl, B., Oberholzer, A., Gust, T., Hostmann, A., Hellmuth, M., Laface, D., Hutchins, B., Laube, G., Veh, R.W., Tschoeke, S.K., Ertel, W., Schulze-Tanzil, G., 2008. IL-10 overexpression differentially affects cartilage matrix gene expression in response to TNF-alpha in human articular chondrocytes in vitro. Cytokine 44, 377–385. https://doi.org/10.1016/j.cyto.2008.10.012.

Nagai, N., Ito, Y., 2014. Effect of solid nanoparticle of indomethacin on therapy for rheumatoid arthritis in adjuvant-induced arthritis rat. Biol. Pharm. Bull. https://doi.org/10.1248/bpb.b13-00917.

Oliveira, R.A., Fierro, I.M., 2018. New strategies for patenting biological medicines used in rheumatoid arthritis treatment. Expert Opin. Ther. Pat. 28, 635–646. https://doi.org/10.1080/13543776.2018.1502748.

Papayannopoulos, V., 2018. Neutrophil extracellular traps in immunity and disease. Nat. Rev. Immunol. 18, 134–147. https://doi.org/10.1038/nri.2017.105.

Pinto, A.C.M.D., de Aguiar Cordeiro, R., Sidrim, J.J.C., de Melo Leite, A.K.R., de Melo Leite, A.C.R., Girão, V.C.C., Brilhante, R.S.N., Rocha, M.F.G., de Queiroz Cunha, F., Rocha, F.A.C., 2013. Anti-inflammatory and immunomodulatory effect of an extract of Coccidioides posadasii in experimental arthritis. Mycopathologia. https://doi.org/10.1007/s11046-013-9621-8.

Rosas, E.C., Correa, L.B., Pádua, T. de A., Costa, T.E.M.M., Mazzei, J.L., Heringer, A.P., Bizarro, C.A., Kaplan, M.A.C., Figueiredo, M.R., Henriques, M.G., 2015. Anti-inflammatory effect of Schinus terebinthifolius Raddi hydroalcoholic extract on neutrophil migration in zymosan-induced arthritis. J. Ethnopharmacol. 175, 490–498. https://doi.org/10.1016/j.jep.2015.10.014.

Ruiz-Miyazawa, K.W., Pinho-Ribeiro, F.A., Borghi, S.M., Staurengo-Ferrari, L., Fattori, V., Amaral, F.A., Teixeira, M.M., Alves-Filho, J.C., Cunha, T.M., Cunha, F.Q., Casagrande, R., Verri, W.A., 2018. Hesperidin methylchalcone suppresses experimental gout arthritis in mice by inhibiting NF-κB activation. J. Agric. Food Chem. 66, 6269–6280. https://doi.org/10.1021/acs.jafc.8b00959.

Sharma, D.C., Shukla, R., Ali, J., Sharma, S., Bajpai, P., Pathak, N., 2016. Phytochemical evaluation, antioxidant assay, antibacterial activity and determination of cell viability (J774 and THP1 alpha cell lines) of P. sylvestris leaf crude and methanol purified fractions. EXCLI J 15, 85–94. https://doi.org/10.17179/excli2015-689.

Sharma, R., Rao, R., Kumar, S., Mahant, S., Khatkar, S., 2018. Therapeutic potential of citronella essential oil: a review. Curr. Drug Discov. Technol. https://doi.org/10.2174/1570163815666180718095041.

Silva, L.A.S., Felix, F.B., Araujo, J.M.D., Souza, E.V., Camargo, E.A., Grespan, R., 2018. Agonistic activity of tamoxifen, a selective estrogen-receptor modulator (SERM), on arthritic ovariectomized mice. Braz. J. Med. Biol. Res. 51, e6799–6804. https://doi.org/10.1590/1414-431X20176799.

Wang, B.C.M., Hsu, P.N., Furnback, W., Ney, J., Yang, Y.W., Fang, C.H., Tang, C.H., 2016. Estimating the economic burden of rheumatoid arthritis in taiwan using the national health insurance database. Drugs. Real World Outcomes. https://doi.org/10.1007/s40801-016-0063-8.

Yamada, A.N., Grespan, R., Yamada, Á.T., Silva, E.L., Silva-Filho, S.E., Damião, M.J., de Oliveira Dalalio, M.M., Bersani-Amado, C.A., Cuman, R.K.N., 2013. Anti-inflammatory activity of Ocimum americanum L. essential oil in experimental model of zymosan-induced arthritis. Am. J. Chin. Med. 41, 913–926. https://doi.org/10.1142/S0192415X13500614.

Zhang, Z., Tsai, P.C., Ramezanli, T., Michniak-Kohn, B.B., 2013. Polymeric nanoparticles-based topical delivery systems for the treatment of dermatological diseases. Wiley Interdiscip. Rev. Nanomedicine Nanobiotechnology. https://doi.org/10.1002/wnan.1211.